Temperature and Concentration Distributions in Fixed-bed Catalytic Reactors : Comparison of Calculated with Experimental Results

AUTHOR(S):

HASHIMOTO, Kenji; TANEDA, Nobuo; HORIGUCHI, Yasuyuki; NAGATA, Shinji

CITATION:

HASHIMOTO, Kenji ...[et al]. Temperature and Concentration Distributions in Fixed-bed Catalytic Reactors : Comparison of Calculated with Experimental Results. Memoirs of the Faculty of Engineering, Kyoto University 1969, 30(4): 541-564

ISSUE DATE:

1969-01-20

URL:

http://hdl.handle.net/2433/280752

Temperature and Concentration Distributions in Fixed-bed Catalytic Reactors: Comparison of Calculated with Experimental Results

By

Kenji HASHIMOTO*, Nobuo TANEDA**, Yasuyuki HORIGUCHI*** and Shinji NAGATA*

(Received June 29, 1968)

Fixed-bed catalytic reactors are most widely used for vapor-phase reactions catalyzed by solid particles. Although theoretical studies concerned with the design method have been extensively performed, few systematic experimental substantiations have been presented. The purpose of this paper is to obtain the necessary data for the reactor design and to evaluate the accuracy of the design method.

The radial temperature profiles and the mean conversions at various catalyst heights were measured in a 5.0 cm I.D. reactor where the hydrogenation of benzene takes place on a nickel-kieselguhr catalyst. The basic design data, the rate of reaction and the heat transfer characteristics in a fixed bed were also presented.

A numerical design method used here is similar to those developed by Smith and Walas with suitable modification. Profiles of temperature and conversion predicted by the numerical method were in good agreement with the experimental data.

1. Introduction

In the chemical industries vapor phase reactions catalyzed by solid catalysts have often been operated in fixed-bed reactors. In most of the catalytic reactions, heat must be removed or supplied through the wall of the reactor tube. Under the nonadiabatic operation, both temperature and concentration variations may be observed in the radial as well as in the longitudinal directions. As a satisfactory design method, three dimensional distributions of temperature and concentration must be taken into account, and several design methods have already been presented. They may be divided into two categories: one is an analytical and the other is a stepwise numerical solution. The analytical solution can be obtained for special cases where the rate term is zero-and first-order with reaspect to temperture and concent-

* Department of Chemical Engineering
** Teijin, Ltd.
*** Department of Chem. Eng., University of Waterloo

ration. However, the rate of reaction is not linear in most cases so that the analytical approaches are not feasible.

A standard procedure of the numerical calculation[1,5,6,11,13,14] is based on the use of a finite difference eqation in place of the partial differential equation. On the other hand, Deans and Lapidus[3] have presented a finite-stage model in which the fixed catalyst bed is imaginarily replaced by a two-dimensional network of perfectly stirred cells[10].

Thus the theoretical analysis of fixed-bed catalytic reactors have been developed in considerable detail. However, few systematic experimental works have been presented for the substantiation of any theoretical design method. Smith and coworkers[12,13] carried out the oxidation of sulfur dioxide and examined the design method. We have presented a simplified design method[7] and compared the calculated with the experimental results[9].

Comparisions are made in this paper between the experimental and calculated results based on a relatively simple numerical method on a highly exothermic reaction, the hydrogenation of benzene to cyclohaxane.

2. Temperature and Conversion Profiles in a Fixed-bed Catalytic Reactor[9]

2.1. Experimental apparatus and procedure

A schematic diagram of the apparatus was shown in Fig. 1. Hydrogen from

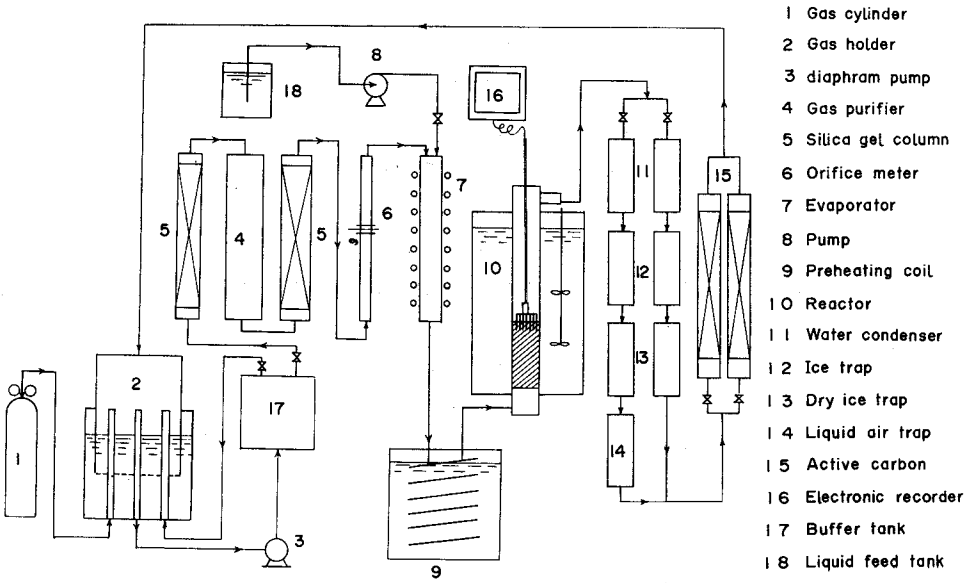

Fig. 1 Schematic diagram of apparatus

a gas cylinder (1) was stored in a gas holder (2) sealed with water, and then sent to an evaporator (7) by a diaphragm pump (3). In order to remove the traces of oxygen and water vapor from hydrogen, the gas was sent through a copper gauze

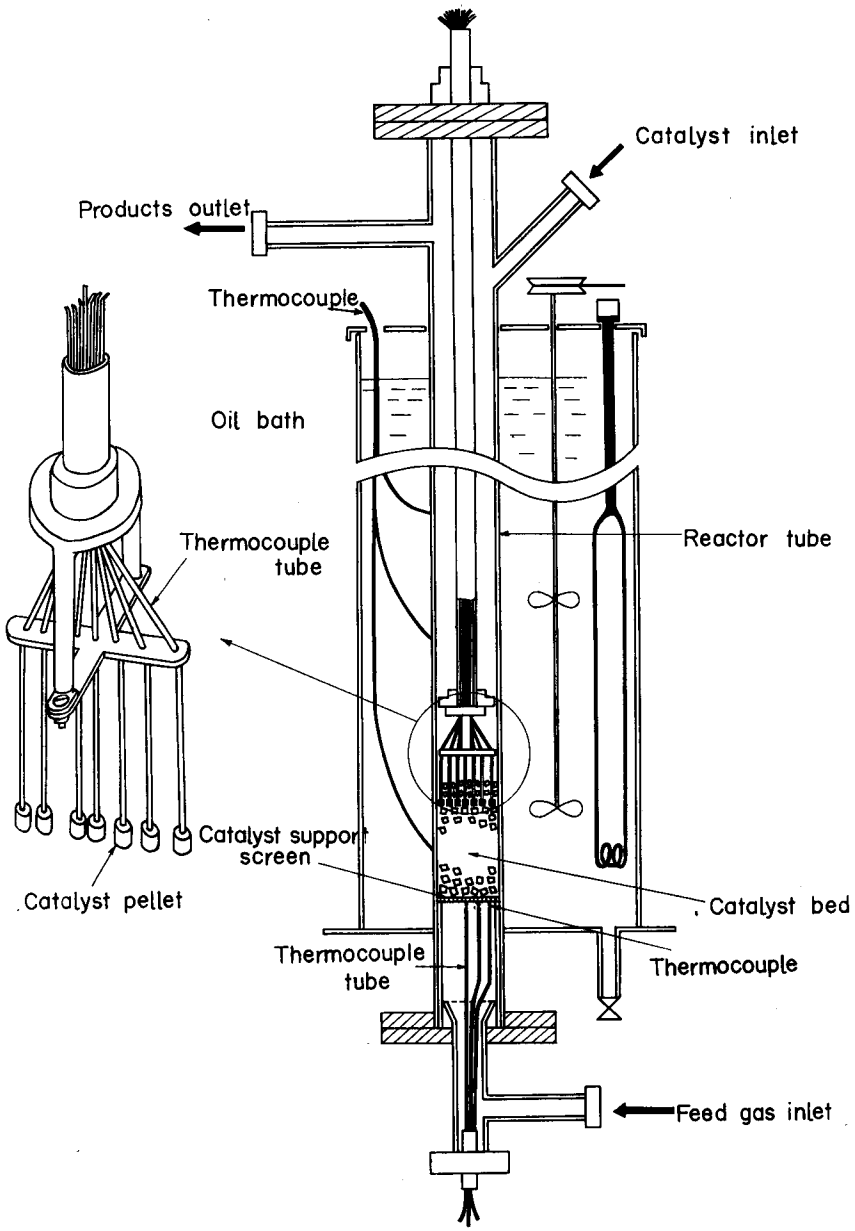

Fig. 2 Detail of fixed-bed catalytic reactor

(4) maintained at 450°C and finally through a silica gel dryer (5). Benzene pumped by a metering pump (8) was vaporized in the evaporator and mixed with hydrogen. From the evaporator the reaction mixture was passed through the coil dipped in the oil bath thermostat (9) and sent into a fixed-bed reactor (10). The fixed-bed catalytic reactor, shown in detail in Fig. 2, consisted of a stainless steel pipe jacketed with machine oil. The reactor tube is 5 cm in diameter and 60 cm in lentgh.

The radial temperature distribution in the catalyst bed at an arbitrary axial position was measured with seven thermocouples in the catalyst pellets. A set of these thermocouples was designed as movable vertically. The radial position of the thermocouples was measured by impressing the thermocouple junctions on a surface of gelatin jelly held on a special holder, which could be slided on the inner wall of the reactor tube.

The effluent from the reactor was cooled in series of cold traps (11)~(14) and separated into condensed products and unreacted hydrogen. Excess hydrogen was recycled to the gas holder passing through a adsorption column (15) packed with active carbon pellets, in which the trace of liquid products was removed.

The liquid product, which consisted mainly of cyclohexane and unreacted benzene, was analyzed by a partition chromatography with a column packed with silicone D.C. 550 stearic acid.

The catalyst used in this work was a commercial nickel catalyst supported on kieselguhr manufactured by Nikki Chemical Co. in Japan, which was found to be more active than that used in the previous work[8]. The catalyst were cylindrical, 3 by 3 mm. The bulk density of the catalyst bed in the reactor was 1200 kg/m^3, the void fraction, 0.325.

The catalyst pellets were packed in height of 2~3 cm higher than the level of thermocouples. It is to be noted that the axial position for the measurement of the radial temperature profile did not coincide with that of mean conversion. The radial temperature profiles and the average conversion of benzene at the different bed heights were observed by repacking the catalyst for each run. The catalysts in the reactor were activated by hydrogen with a space velocity of 2000 [1/hr] for 3 hours. The reactor wall was maintained at 100°C, and the inlet gas temperature at the center of the tube was fixed at 125°C in all experiments.

2.2. Experimental results

Both the conversion and the radial temperature profile were experimentally measured in the range of catalyst bed height of 1 to 43 cm, and in mass velocity of 227 to 1010 kg/m^2. hr at the ratio of 20 to 60 in molar flow rate of hydrogen to benzene at the reactor inlet. In order to avoid unstable operation due to highly

exothermic reaction, the feed stream was diluted by a large excess hydrogen.

The radial temperature profiles at several catalyst bed levels are illustrated in Fig. 3. The longitudinal temperature distributions are shown in Fig. 5 and Fig. 6, and the mean conversion in Fig. 7. The entering gas temperature was 125°C, and the wall of the reactor was maintained at 100°C in the oil bath.

A few byproducts were found when the maximum temperature of the catalyst bed exceeded about 250°C. No cyclohexene was detected in the present work. Impurities in the total liquid products were less than 0.5%, so that the effects of side reactions on the temperature and conversion would be negligible.

An attempt was made to measure the temperature difference between gas and

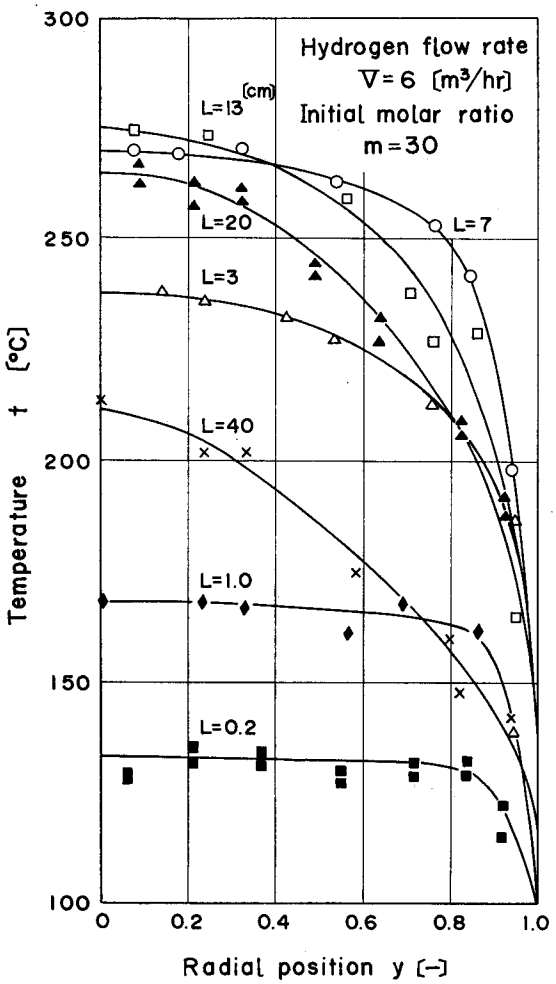

Fig. 3 Radial temperature distributions in reactor

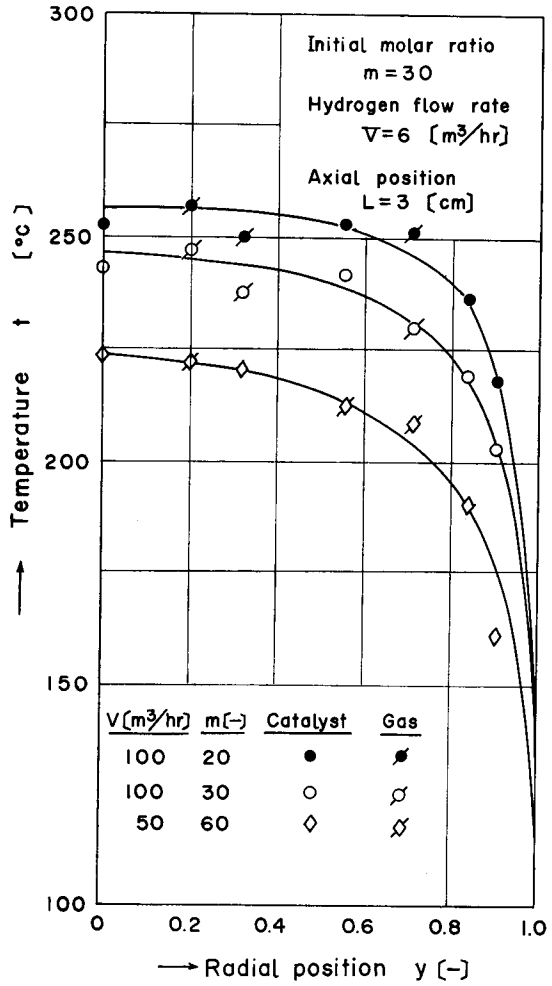

Fig. 4 Temperature difference between catalyst particles and gas

catalyst particle in the bed. Three thermocouples were insetred in the gas phase to measure gas temperature. As shown in Fig. 4, negligible difference in temperature was found between gas and catalysts. According to the calculation formula proposed by Yoshida *et al*[15], the difference in temperature was also less than 2.5°C.

3. Reaction Kinetics of the Hydrogenation of Benzene

Kinetic studies of the hydrogenation of benzene to cyclohexane have extensively been performed on a variety of catalysts, and the commerical plants have

already been in operation. Useful data, however, are not available for the reasonable design of catalytic reactors.

In the previous paper the following reaction rate equation has been presented[8]:

$$r = \frac{kK_H{}^3K_B p_H{}^3 p_B}{(1+k_H p_H+K_B p_B+K_C p_C)^4} \tag{1}$$

where k is the rate constant, K's the adsorption equilibrium constants, and p's partial pressures of the components. These quantities were given as the function of temperature. In the present work the rate data were measured again. The experimental apparatus and procedure are essentially the same as those used in the previous work. The initial rates were measured in the following range of conditions. Reaction temperautre, $t=120\sim250°C$, partial pressure of benzene, $p_B=0.02\sim0.11$ atm, Reynolds number, $Re_p=22\sim52$.

It is assumed that Eq.(1) is applicable for the new catalyst, values of adsorption equilibrium constants are equal for both catalysts, and the difference in activity is mainly confined to the rate constant k. The rate constants derived from the above assumption can be correlated by the following equation of Arrhenius type:

$$\ln k = -\frac{12{,}100}{RT}+\frac{32.3}{R} \tag{2}$$

The adsorption equilibrium constants obtained in the previous paper are as follows:

$$\left.\begin{aligned}\ln K_H &= \frac{15{,}500}{RT}-\frac{31.9}{R}\\ \ln K_B &= \frac{11{,}200}{RT}-\frac{23.1}{R}\\ \ln K_C &= \frac{8{,}900}{RT}-\frac{19.4}{R}\end{aligned}\right\} \tag{3}$$

Let m represent the molar ratio of hydrogen to benzene at the reactor inlet, then the partial pressures may be written in terms of m, the conversion of benzene f and the total pressure P_t

$$\left.\begin{aligned}p_H &= P_t(m-3f)/(1+m-3f)\\ p_B &= P_t(1-f)/(1+m-3f)\\ p_C &= P_t f/(1+m-3f)\end{aligned}\right\} \tag{4}$$

By substituting Eqs. (2)~(4) into Eq.(1) the rate eqation is expressed as a function of conversion and temperature.

4. Heat Transfer Characteristics in Catalyst Bed[4]

The heat transfer phenomena in fixed bed catalytic reactors may usually be analyzed by means of a radial effective thermal conductivity k_e and the heat transfer coefficient at a reactor wall h_w. These values were measured in the same reactor as that used for the temperature and conversion measurements.

The experimental results were correlated by the following equations. As the reactor was operated under the condition of large excess in hydrogen, the heat transfer characteristics of hydrogen were used in place of reaction mixture.

$$k_e/k_g = 1.0+0.13\,\mathrm{Pr}\cdot\mathrm{Re}_p$$
$$h_w d_p/k_g = 0.5+0.068\,\mathrm{Pr}\cdot\mathrm{Re}_p$$

5. Mathematical Model of Fixed-bed Catalytic Reactors

For simplicity we shall assume the catalyst bed as a quasi-homogeneous system, that is, concentration and temperature vary smoothly and continuously in the catalyst bed.

The following basic assumptions are made for the mathematical analysis of a fixed-bed catalytic reactor:

(1) the fluid and solid temperatures are substantially equal at any point.

(2) the axial conduction and diffusion are negligible.

(3) the velocity in the cross section of the reactor is uniform.

(4) the physical properties of the gas are invarialbe throughout the reactor.

With these assumptions a set of partial differential equations describing enthalpy and mass transport are derived for the stationary state.

$$-\frac{\partial t}{\partial L}+\frac{k_e}{Gc_p}\left(\frac{\partial^2 t}{\partial R^2}+\frac{1}{R}\frac{\partial t}{\partial R}\right)+\frac{r\rho_B(-\Delta H)}{Gc_p}=0$$
$$-\frac{\partial f}{\partial L}+\frac{D_e}{u}\left(\frac{\partial^2 f}{\partial R^2}+\frac{1}{R}\frac{\partial f}{\partial R}\right)+\frac{rM_{av}}{Gy_0}=0$$

The initial and the boundary conditions are

$$\text{at}\quad L=0 \quad : \quad t=t_0 \ \ (\text{const})$$
$$f=f_0 \ \ (\text{const})$$
$$\text{at}\quad R=0 \quad : \quad \partial t/\partial R=0$$
$$\partial f/\partial R=0$$

$$\text{at} \quad R = R_w \quad : \quad -k_e(\partial t/\partial R) = h_w(t - t_w)$$
$$\partial f/\partial R = 0$$

Before proceeding further, the following transformations of variables are introduced:

$$h = h_w R_w/k_e, \quad x = L/R_w, \quad y = R/R_w, \quad \alpha = \rho_B(-\Delta H)R_w/Gc_p,$$
$$\beta = \rho_B M_{av} R_w/Gy_0, \quad \delta = D_e\rho_f/GR_w, \quad \kappa = k_e/Gc_pR_w.$$

Thus the basic equations are given as follows:

$$-\frac{\partial t}{\partial x} + \kappa\left(\frac{\partial^2 t}{\partial y^2} + \frac{1}{y}\frac{\partial t}{\partial y}\right) + \alpha r = 0 \tag{5}$$

$$-\frac{\partial f}{\partial x} + \delta\left(\frac{\partial^2 f}{\partial y^2} + \frac{1}{y}\frac{\partial f}{\partial y}\right) + \beta r = 0 \tag{6}$$

The transformed initial and boundary conditions are listed below:

$$\text{At} \quad x = 0 \quad : \quad t = t_0 \tag{7}$$
$$f = f_0 \tag{8}$$
$$\text{At} \quad y = 0 \quad : \quad \partial t/\partial y = 0 \tag{9}$$
$$\partial f/\partial y = 0 \tag{10}$$
$$\text{At} \quad y = 1 \quad : \quad \partial t/\partial y + h(t - t_w) = 0 \tag{11}$$
$$\partial f/\partial y = 0 \tag{12}$$

6. Numerical Solutions of Temperature and Conversion Distributions

6.1. Finite difference equations

The equations are parabolic type. The numerical method used here is similr to those presented by Smith[13] and Walas[14]. They suggested forward difference apporximations for both the axial and the radial derivatives, whereas in the present work radial derivatives are approximated by central difference formulas because of their lower truncation errors. Uses of central differences for the axial derivatives in the parabolic type always lead to unstable solutions, so that forward differences are used for the axial derivatives.

If w and l represent the number of the increments in the radial and axial directions respectively, and Δy *and* Δx their magnitude, then

$$\left.\begin{aligned} y &= m\Delta y, \qquad m = 0, 1, 2, \cdots\cdots, w \\ x &= n\Delta x, \qquad n = 0, 1, 2, \cdots\cdots, l \end{aligned}\right\} \tag{13}$$

If the cylindrical bed is divided into such increments, and the temperature at the grid point $[m, n]$ i. e at $y=m\Delta y$ and $x=n\Delta x$ is represented by $t_{m,n}$, the partial derivatives in the basic equaions are represented by the following equations:

$$\frac{\partial t}{\partial x} = \frac{t_{m,n+1}-t_{m,n}}{\Delta x} \tag{14}$$

$$\frac{\partial t}{\partial y} = \frac{t_{m+1,n}-t_{m-1,n}}{2\Delta y} \tag{15}$$

$$\frac{\partial^2 t}{\partial y^2} = \frac{t_{m+1,n}-2t_{m,n}+t_{m-1,n}}{(\Delta y)^2} \tag{16}$$

Since the rate is varied between the increment n to $n+1$, the reaction rates are substituted by the arithmetic average value,

$$r = \frac{r_{m,n}+r_{m,n+1}}{2}$$

At the central axis of the reactor tube, the term $(1/y)\cdot(\partial t/\partial y)$ becomes indeterminate, therefore, it is replaced by the following relationship:

$$\lim_{y\to 0}\frac{1}{y}\frac{\partial t}{\partial y} = \frac{\partial^2 t}{\partial y^2}$$

At the wall the radial derivative of temperature is approximated by the forward-difference equation. On the other hand, since the concentration gradient is zero at the wall, the conversion profile can be regarded as symmetric to the wall and the following substitution can be made:

$$f_{w+1,n} = f_{w-1,n}$$

Futhermore, it is convenient to introduce two dimensionless parameters M and N, which are defined as follows. The parameter M is called a modulus of heat transfer, and N a modulus of mass transfer.

$$M = \frac{(\Delta y)^2}{\kappa \Delta x} \tag{18}$$

$$N = \frac{(\Delta y)^2}{\delta \Delta x} \tag{19}$$

With these preparations, the set of partial differential equations are approximately replaced by a set of finite difference equations:

At the center:

$$t_{0,n+1} = t_{0,n} + \frac{4}{M}(t_{1,n}-t_{0,n}) + \frac{\alpha \Delta x}{2}(r_{0,n}+r_{0,n+1}) \tag{20}$$

$$f_{0,n+1} = f_{0,n} + \frac{4}{M}(f_{1,n} - f_{0,n}) + \frac{\beta \Delta x}{2}(r_{0,n} + r_{0,n+1}) \tag{21}$$

At intermediate radial positions $(0 < m < w)$:

$$t_{m,n+1} = t_{m,n} + \frac{1}{M}\left[\left(1 + \frac{1}{2m}\right)t_{m+1,n} - 2t_{m,n} + \left(1 - \frac{1}{2m}\right)t_{m-1,n}\right] + \frac{\alpha \Delta x}{2}(r_{m,n} + r_{m,n+1}) \tag{22}$$

$$f_{m,n+1} = f_{m,n} + \frac{1}{N}\left[\left(1 + \frac{1}{2m}\right)f_{m+1,n} - 2f_{m,n} + \left(1 - \frac{1}{2m}\right)f_{m-1,n}\right] + \frac{\beta \Delta x}{2}(r_{m,n} + r_{m,n+1}) \tag{23}$$

At the wall:

$$t_{w,n+1} = \frac{t_{w-1,n+1} + t_w h \Delta y}{1 + h y} \tag{24}$$

$$f_{w,n+1} = f_{w,n} + \frac{2}{N}(f_{w-1,n} - f_{w,n}) + \frac{\beta \Delta x}{2}(r_{w,n} + r_{w,n+1}) \tag{25}$$

It is seen that these equations involve reaction rates at the axial increment $n+1$. Consequently, the solution will require iteration prodceure in which $r_{m,n+1}$ is to be assumed in the first trial and subsequently replaced by the better value obtained at the end of the first trial.

6.2. Stability of solution

For the explicit forward-difference equation the stability of the solution may be highly influenced by the selection of the value of the modulus. As the criterion of the stability of non-linear equations has not yet been established, the computation for a few values of the modulus were carried out. It was found that the numerical solution in this case would be performed with enough stability if we select the modulus of heat transfer larger than 2.5.

6.3. Convergence of solution

The effect of the radial step size on truncation error was examined by varying three different sizes for the same inlet condition. Calculations were made with the experimental run corresponding $V = 6.0$ and $m = 30$. In these computations the value of M is fixed at 4.0. Therefore, it is noted that considerable variation results also in the longitudinal step size. The computed results were listed in Table 1. There is definitely some truncation error in t and f, which accumulates at the end of the reactor. The relative error in t is higher than that in f. The maximum error between 10 points and 20 points in the radial direction is within 0.5%, so

Table 1. Effect of the size of radial increment on computed values

(Modulus of heat transfer is fixed at 4.0)

Axial position [cm]	No. of radial div.	Temperature			Conversion		
		y=0.0	y=0.5	mean	y=0.0	y=0.5	mean
6.6	6	257.20	253.15	232.20	0.6488	0.6661	0.7303
	10	256.87	253.39	234.19	0.6471	0.6640	0.7326
	20	256.85	253.66	235.64	0.6468	0.6631	0.7314
33.0	6	224.03	195.08	172.92	0.9836	0.9973	0.9974
	10	225.37	196.33	173.86	0.9817	0.9970	0.9971
	20	226.56	197.39	174.66	0.9800	0.9966	0.9969

Table 2. The effect of the modulus of heat transfer on computed values.

(Δy=0.1)

Axial position [cm]	M[—]	Temperature			Conversion		
		y=0.0	y=0.9	mean	y=0.0	y=0.9	mean
31.7	2.5	230.41	147.52	177.04	0.97205	0.99903	0.99560
	3.0	230.38	147.53	177.05	0.97213	0.99904	0.99562
	4.0	230.34	147.54	177.05	0.97223	0.99905	0.99564
	5.0	230.31	147.55	177.05	0.97230	0.99906	0.99566

that it is considered that 10 points are adequate for engineering calculation.

The effect of the axial step size on truncation was also checked for four values of M and listed in Table 2. It is clear that the axial step size gives little influence on truncation error.

7. Comparison of Experimental and Calculated Results

Using Eqs. (20)~(25), temperatures and conversions were calculated on a digital computer at six mass velocities for comparison with the expermental results. In these calculations the radius of the reactor tube was divided into ten radial increments, i.e., Δy=0.1, and the modulus of heat transfer M was taken as 4.0. Then the increment of the longitudinal direction Δx was fixed by Eq. (18). The mean temperatures and conversions at any cross section of the tube were computed by the Simpson formula.

Table 3. Data used in calculation

Run No.	1	2	3	4	5	6
V [m³/hr]	7.5	7.5	6.0	6.0	3.0	3.0
m [—]	20	30	20	30	30	60
G [kg/m²·hr·°C]	1010	788	808	631	315	227
Re_p [—]	61.0	49.5	48.8	39.6	19.8	14.6
$Pe_r=ud_p/D_e$ [—]	12.8	12.8	12.8	12.6	11.8	11.8
k_e [kcal/m·hr·°C]	0.770	0.756	0.657	0.650	0.435	0.437
h_w [kcal/m²·hr·°C]	133	130	113	112	74.1	74.3
α [gr·hr·°C/gr-mol]	1016.6	1077.6	1270.3	1345.7	2695.7	2880.0
β [gr·hr/gr-mol]	3.518	5.276	4.397	6.580	13.20	26.31
κ [—]	0.02119	0 02205	0.02260	0.02365	0.03175	0.03407
δ [—]	0.009348	0.009348	0.009348	0.009506	0.01020	0.0102
w [—]	10	10	10	10	10	10
M [—]	4.0	4.0	4.0	4.0	4.0	4.0
N [—]	9.068	9.436	9.671	9.965	12.45	13.36
$\Delta L=\Delta z/R_w$ [cm]	0.295	0.283	0.277	0.264	0.197	0.183

The reaction rates and the heat transfer characteristics obtained in the above sections were used. The values of the radial effective diffusivity were evaluated by the chart presented by Bernard and Wilhelm[2]. Numerical values required for the calculations are summarized in Table 3.

Observed and computed temperatures are shown in Fig. 5 for the centeral axis and for the mean, and in Fig. 6 for two radial positions. Comparisons of mean conversions with experimental data are indicated in Fig. 7. In view of the complexity of the problem, it may be said the agreement between the calculated with the experimental results for both temperature and conversion is pretty good. In the greater part of the reactor, the calculated values of temperature show little lower values than those observed. It may be considered that this discrepancy is mainly caused by the uncertainty in kinetic data. It is particularly interesting to note that the computed conversions at radial positions of $y=0.9$ except near the inlet region of the reactor are higher than those at the center. This may be due to the temperature dependency of the hydrogenation of benzene. The reaction rate shows a maximum on the temperature range of 180 to 200°C. When the temperature at the center exceeds 200°C, the conversion rate is lower than that in the vicinity of the reactor wall.

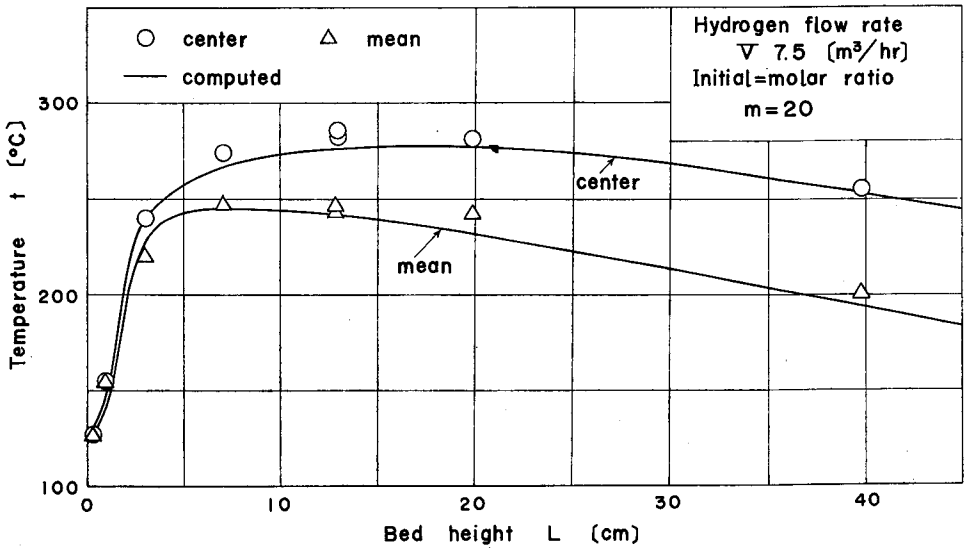
○ center △ mean
— computed
Hydrogen flow rate
V 7.5 [m³/hr]
Initial=molar ratio
m=20
center
mean
Temperature t [°C]
300
200
100
0
10
20
30
40
Bed height L [cm]

(A)

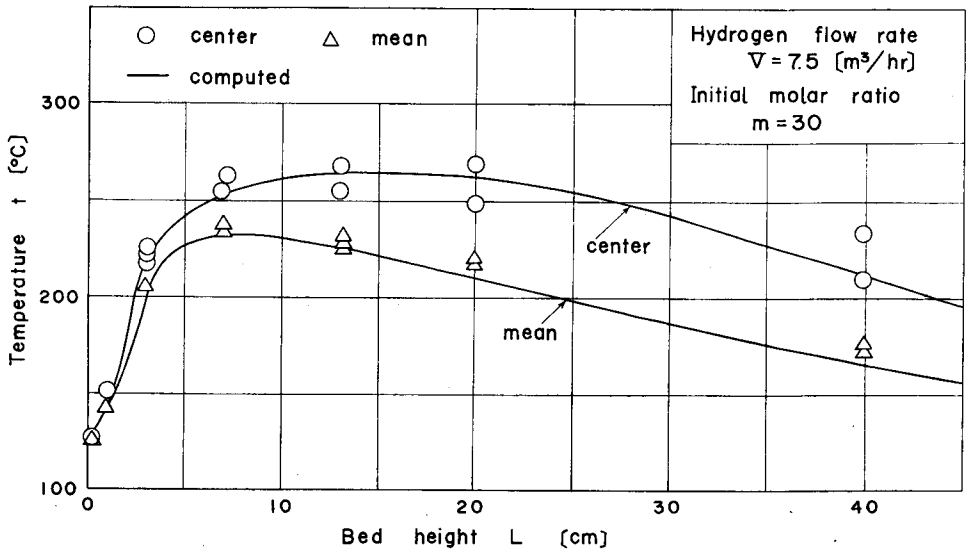
○ center △ mean
— computed
Hydrogen flow rate
V=7.5 [m³/hr]
Initial molar ratio
m=30
center
mean
Temperature t [°C]
300
200
100
0
10
20
30
40
Bed height L [cm]

(B)

Fig. 5

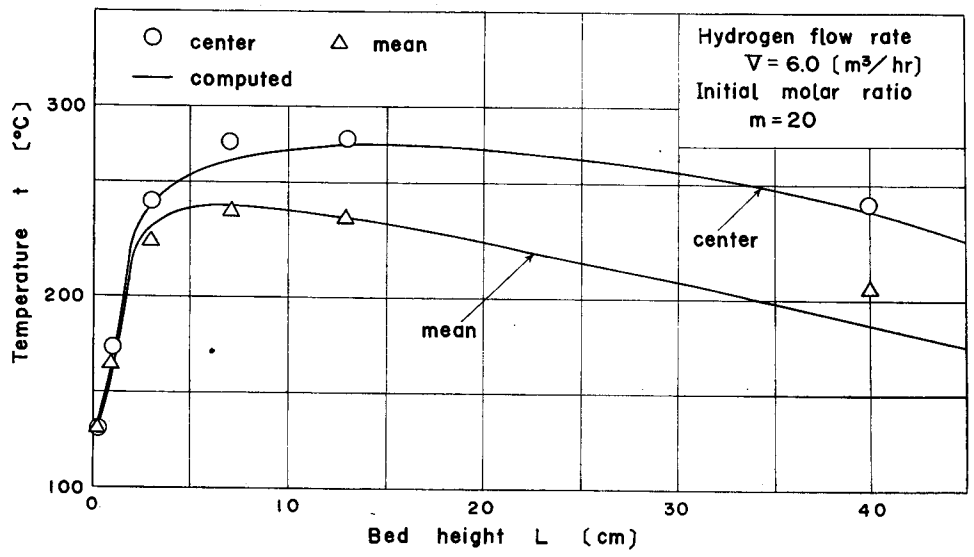
center
mean
computed
Hydrogen flow rate
V = 6.0 (m³/hr)
Initial molar ratio
m = 20
center
mean
Temperature t (°C)
300
200
100
0
10
20
30
40
Bed height L (cm)

(C)

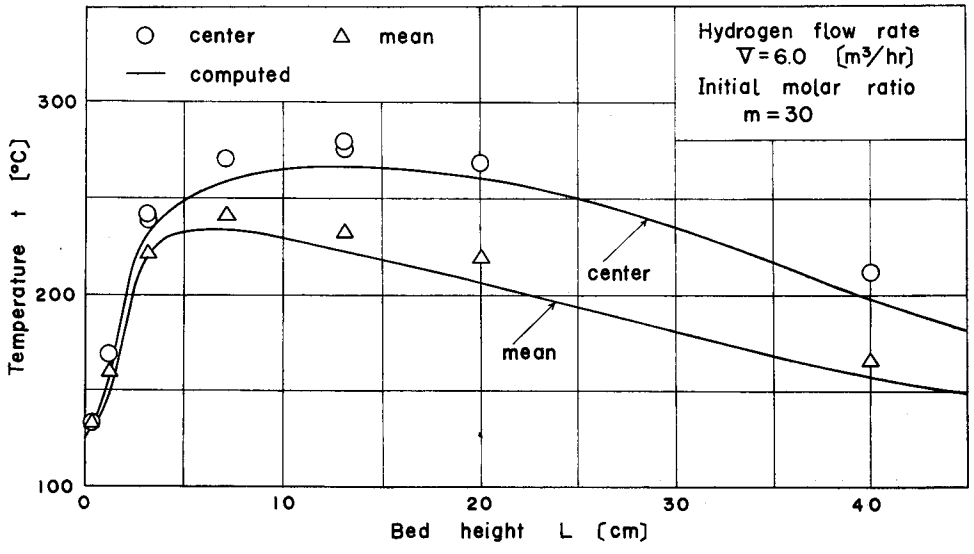
center
mean
computed
Hydrogen flow rate
V = 6.0 (m³/hr)
Initial molar ratio
m = 30
center
mean
Temperature t (°C)
300
200
100
0
10
20
30
40
Bed height L (cm)

(D)

Fig. 5

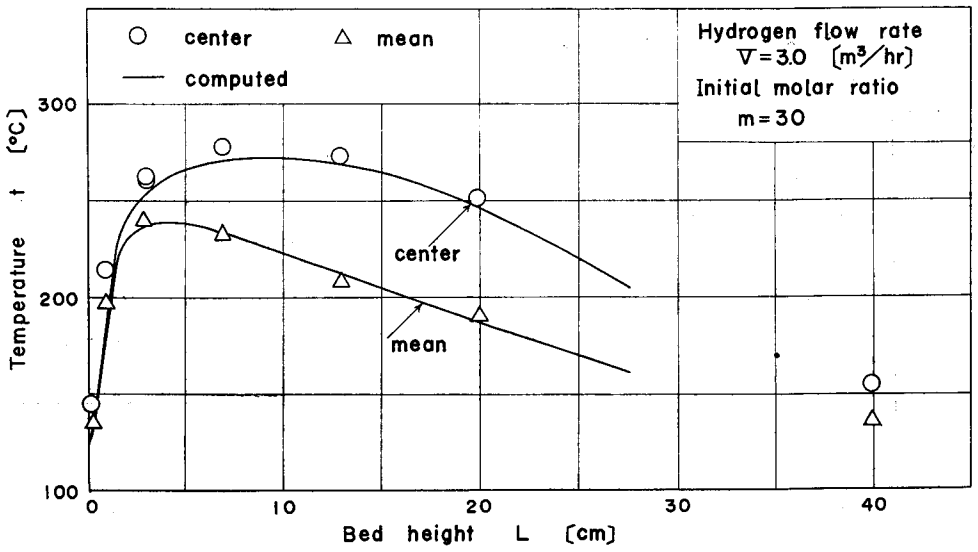

(E)

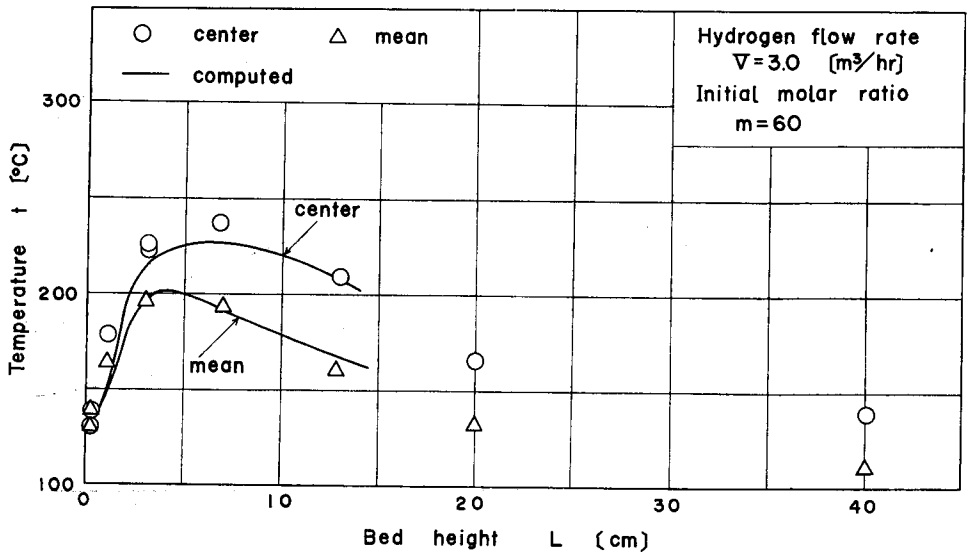

(F)

Fig. 5 (A, B, C, D, E, F) Comparison of experimental and calculated temperature distributions

(for the central axis and for the mean)

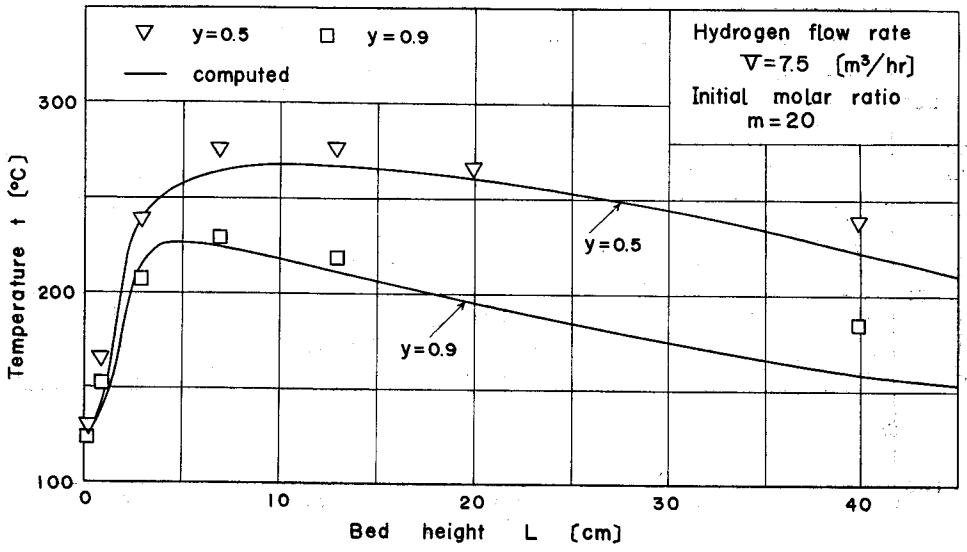
▽ y=0.5
□ y=0.9
computed
Hydrogen flow rate
▽=7.5 [m³/hr]
Initial molar ratio
m=20
y=0.5
y=0.9
Temperature t [°C]
300
200
100
0
10
20
30
40
Bed height L [cm]

(A)

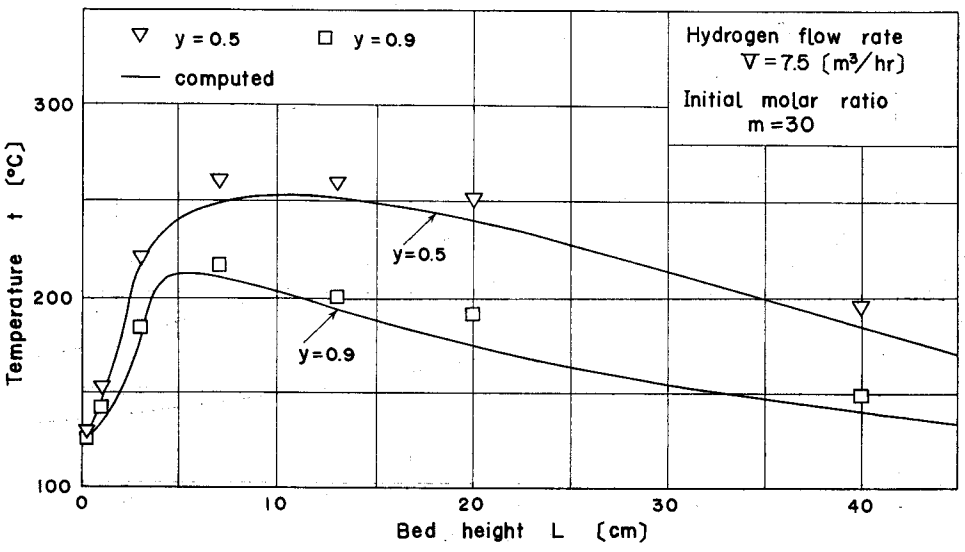
▽ y=0.5
□ y=0.9
computed
Hydrogen flow rate
▽=7.5 [m³/hr]
Initial molar ratio
m=30
y=0.5
y=0.9
Temperature t [°C]
300
200
100
0
10
20
30
40
Bed height L [cm]

(B)

Fig. 6

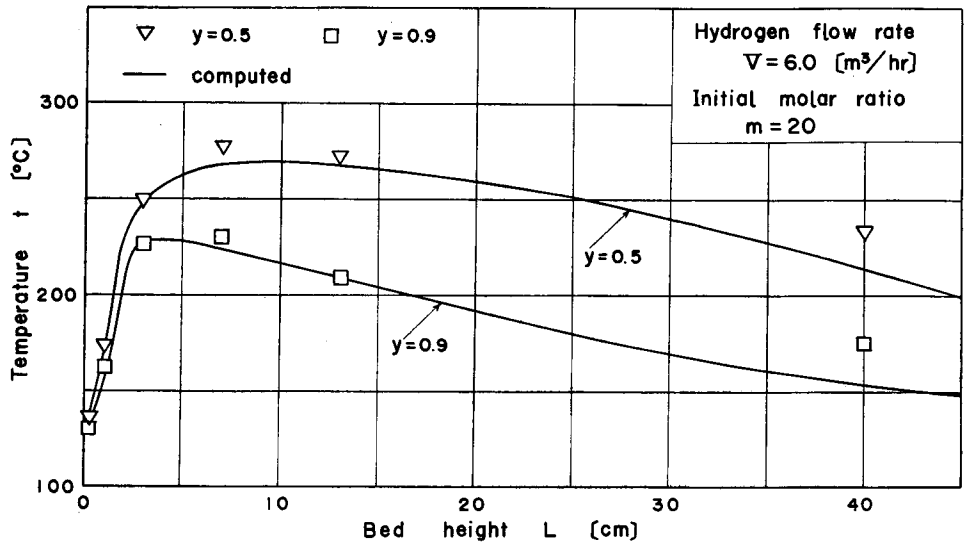
y=0.5
y=0.9
computed
Hydrogen flow rate
∇=6.0 [m³/hr]
Initial molar ratio
m=20
Temperature t [°C]
300
200
100
0
10
20
30
40
Bed height L [cm]
y=0.5
y=0.9

(C)

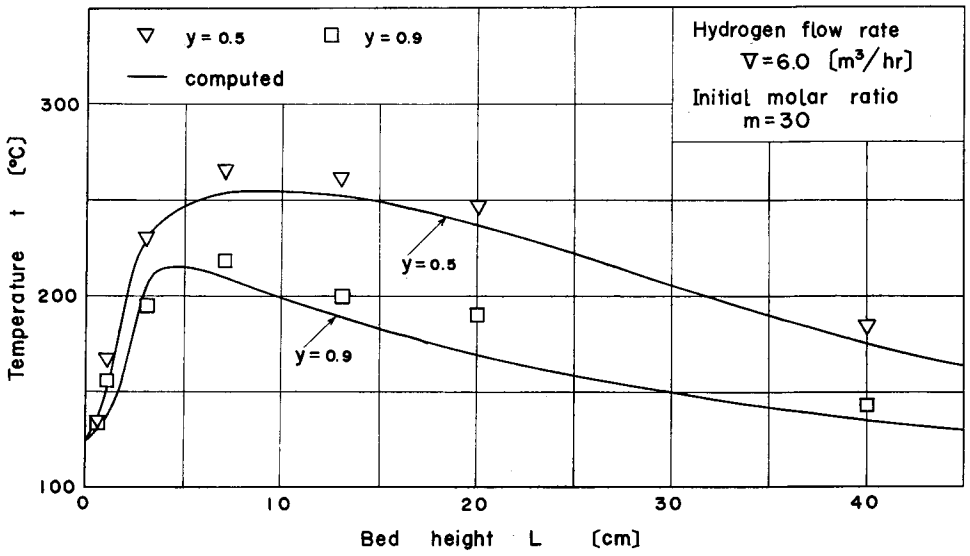
y=0.5
y=0.9
computed
Hydrogen flow rate
∇=6.0 [m³/hr]
Initial molar ratio
m=30
Temperature t [°C]
300
200
100
0
10
20
30
40
Bed height L [cm]
y=0.5
y=0.9

(D)

Fig. 6

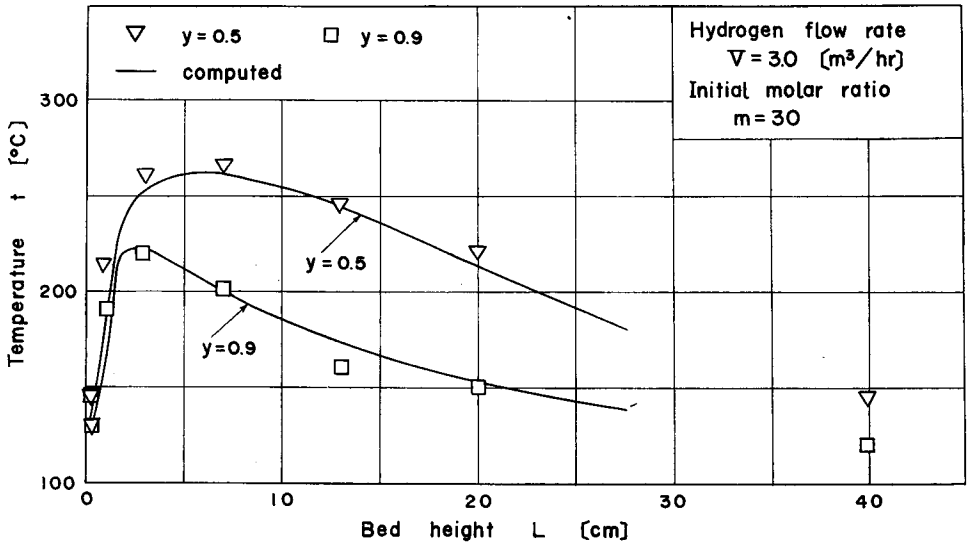

(E)

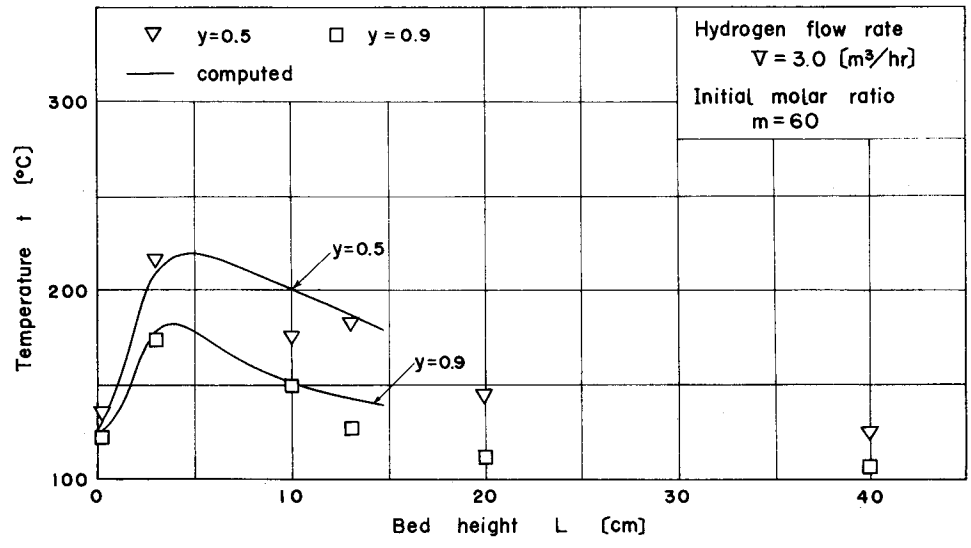

(F)

Fig. 6 (A, B, C, D, E, F) Comparison of experimental and calculated temperature distributions

(for $y=0.5$ and $y=0.9$)

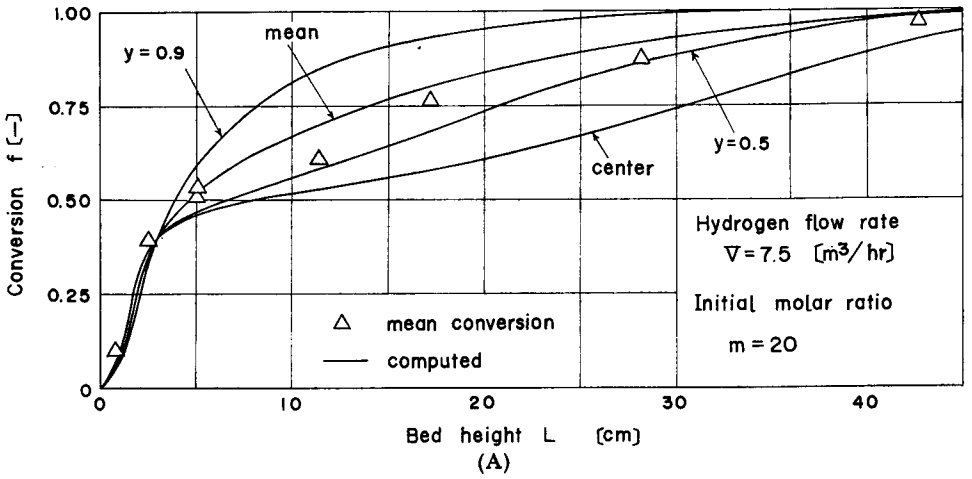
1.00
0.75
0.50
0.25
0
Conversion f [-]
y = 0.9
mean
y=0.5
center
Hydrogen flow rate
V=7.5 [m³/hr]
Initial molar ratio
m = 20
mean conversion
computed
0
10
20
30
40
Bed height L [cm]

(A)

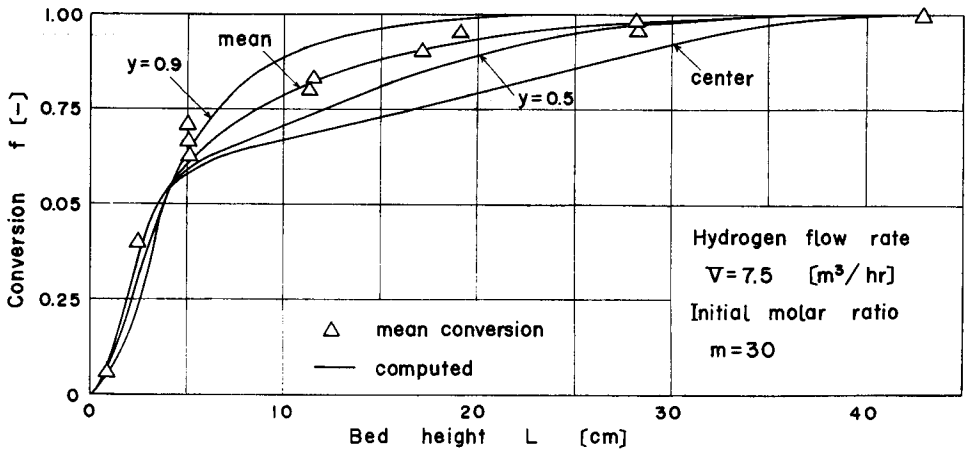
1.00
0.75
0.05
0.25
0
Conversion f [-]
y=0.9
mean
y=0.5
center
Hydrogen flow rate
V=7.5 [m³/hr]
Initial molar ratio
m=30
mean conversion
computed
0
10
20
30
40
Bed height L [cm]

(B)

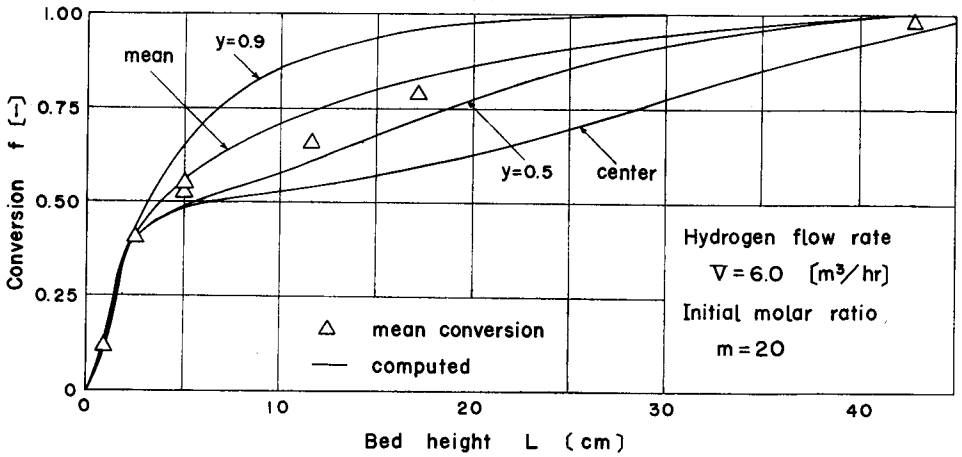
1.00
0.75
0.50
0.25
0
Conversion f [-]
mean
y=0.9
y=0.5
center
Hydrogen flow rate
V=6.0 [m³/hr]
Initial molar ratio
m=20
mean conversion
computed
0
10
20
30
40
Bed height L (cm)

(C)

Fig. 7

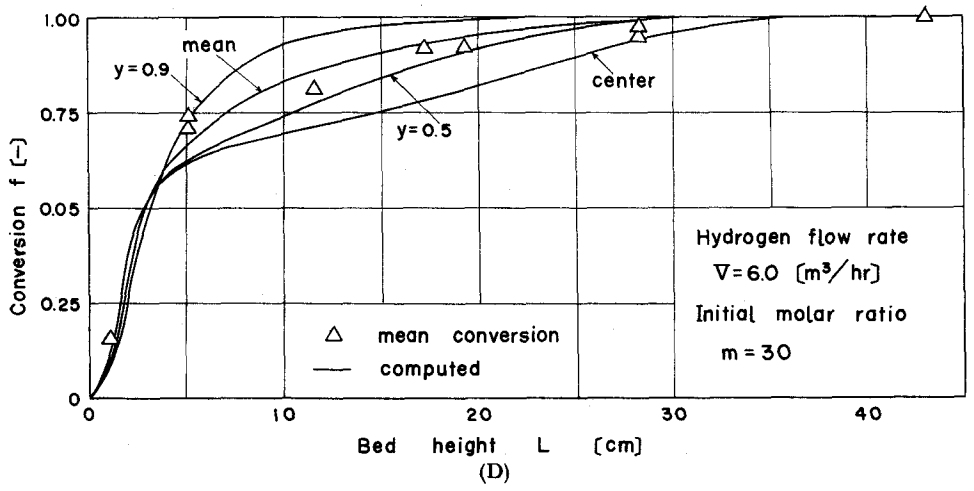

(D)

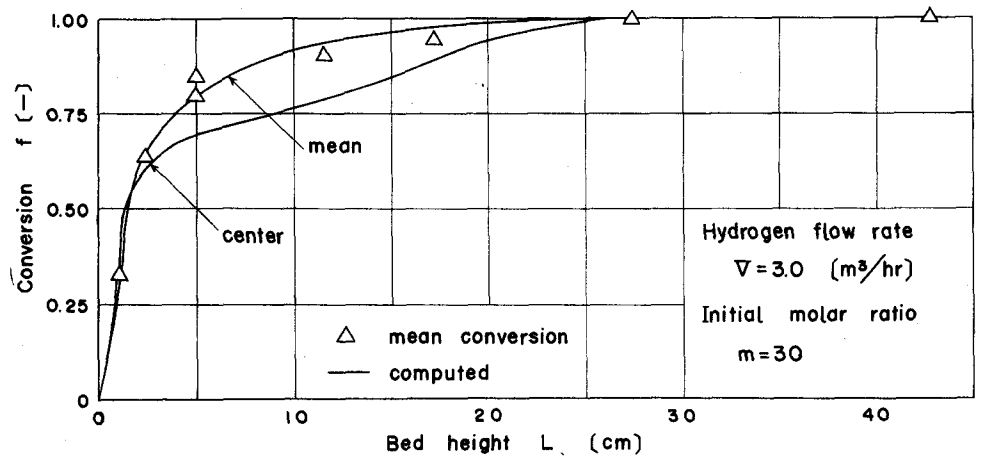

(E)

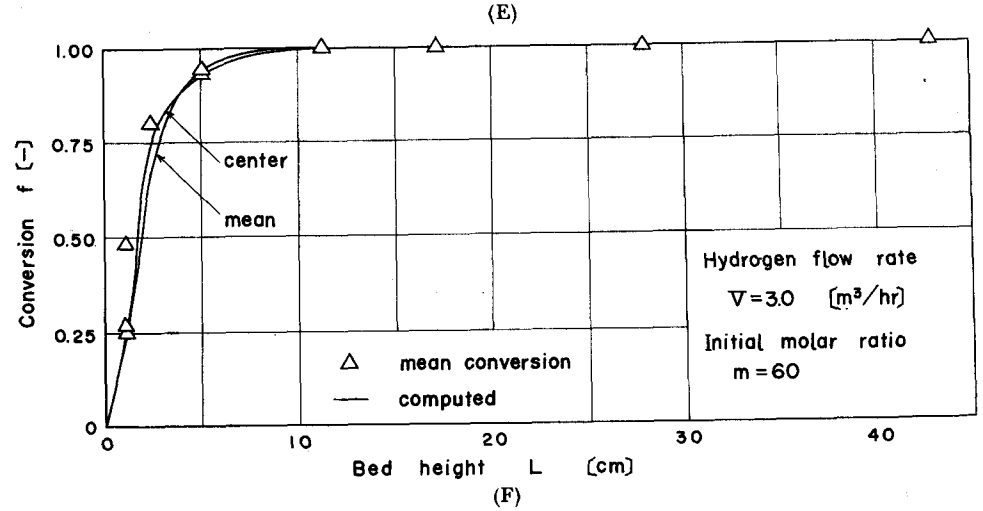

(F)

Fig. 7 (A, B, C, D, E, F) Comparison of experimental and calculated conversion distributions

8. Conclusion

The temperature and conversion distributions were precisely measured in the fixed-bed catalytic reactor in which the hydrogenation of benzene to cyclohexane took place. The studies on the kinetics and the heat transfer were also carried out.

On the other hand, finite difference equations were derived by modifying the method of Smith-Walas.

The calculated temperature and conversion profiles showed good agreement with the experimental results. Therefore, the simplified numerical model for fixed-bed catalytic reactors is very useful for the reactor design.

Nomenclature

c_p	:	specific heat at constant pressure	[kcal/kg·°C]
D_e	:	radial effective diffusivity in fixed bed	[m²/hr]
d_p	:	effective diameter of catalyst particles	[mm] or [m]
f	:	fractional conversion of limiting component in reactants	[—]
G	:	superficial mass velocity of fluid	[kg/m²·hr]
ΔH	:	heat of reaction	[cal/gr-mol]
h	:	$h_w R_w/k_e$	[—]
h_w	:	heat transfer coefficient at reactor tube wall	[kcal/m²·hr·°C]
K	:	adsorption equilibrium constant	[1/atm]
k	:	reaction rate constant	[gr-mol/gr·hr]
k_e	:	radial effective thermal conductivity	[kcal/m·hr·°C]
k_g	:	thermal conductivity of fluid	[kcal/m·hr·°C]
L	:	longitudinal distance in reactor	[cm] or [m]
l	:	number of axial increments, Δy	[—]
M	:	modulus of radial heat transfer, $(\Delta y)^2/\kappa \cdot \Delta x$	[—]
M_{av}	:	average molecular weight of fluid	[gr/gr-mol]
m	:	molar ratio of hydrogen to benzene at reactor inlet	[—]
m	:	index of radial increment	[—]
N	:	modulus of radial mass transfer, $(\Delta y)^2/\delta \cdot \Delta x)$	[—]
n	:	index of axial increment	[—]
Pe	:	Peclet number, $\mathrm{Pe}=\mathrm{Pr}\cdot\mathrm{Re}_p=c_p d_p G/k_g$	[—]
Pe_r	:	modified Peclet number, $\mathrm{Pe}_r=ud_p/D_e$	[—]
Pr	:	Prandtl number, $\mathrm{Pr}=c_p\eta/k_g$	[—]
Pt	:	total pressure	[atm]

p	:	partial pressure	[atm]
R	:	radial distance in reactor	[cm] or [m]
R	:	gas constant, 1.987	[cal/g-mol·°K]
Re_p	:	Reynolds number, $Re_p = Gd_p/\eta$	[—]
R_w	:	radius of reactor tube	[cm] or [m]
r	:	reaction rate	[gr-mol/gr·hr]
T	:	temperature	[°K]
t	:	temperature	[°C]
$t_{m,n}$	:	temperature at grid point $[m, n]$	[°C]
u	:	superficial linear velocity	[m/hr]
V	:	volumetric flow rate of hydrogen at reactor inlet (N.T.P.)	[m³/hr]
w	:	number of radial increments, Δx	
x	=	L/R_w	[—]
y	=	R/R_w	[—]
y_0	:	mole fraction of limiting component in feed stream	[—]
α	=	$\rho_B(-\Delta H)R_w/Gc_p$	[gr·hr·°C/gr-mol]
β	=	$\rho_B M_{av} \cdot R_w/Gy_0$	[gr·hr/gr-mol]
δ	=	$D_e\rho_f/GR_w$	[—]
η	:	viscosity of fluid	[kg/m·hr]
κ	=	k_e/Gc_pR_w	[—]
ρ_B	:	bulk density of catalyst bed	[kg/m³]
ρ_f	:	density of fluid	[kg/m³]

Subscript

B	:	benzene
C	:	cyclohexane
H	:	hydrogen
o	:	entrance of reactor
w	:	inner wall of reactor

References

1) Beek, J.: "Advances in Chemical Engineering," Vol. 3, p. 203, Academic Press, N. Y., (1962).
2) Bernard, R.A. and R.H. Wilhelm: *Chem. Eng. Progr.*, **46**, 233 (1950).
3) Deans, H.A. and L. Lapidus: *A. I. Ch. E. Journal*, **6**, 656, 663 (1960).
4) Hashimoto, K., N. Suzuki, M. Teramoto and S. Nagata: *Kagaku Kogaku* (*Chem. Eng., Japan*), **29**, 672 (1965), *Kagaku Kogaku* (Abridged Edition), **4**, 68 (1966).
5) Kubota, H. and T. Akehata: *Kagaku Kogaku* (*Chem. Eng., Japan*), **28**, 284 (1964).
6) Mickley, H.S. and R.W. Letts: *Can. J. Chem. Eng.*, **41**, 273 (1963), **42**, 21 (1964).
7) Nagata, S., K. Hashimoto, I. Taniyama and H. Nishida: *Kagaku Kogaku* (*Chem. Eng., Japan*), **26**, 569 (1962).

8) Nagata, S., K. Hashimoto, I. Taniyama, H. Nishida and S. Iwane: *Kagaku Kogaku* (*Chem. Eng., Japan*), **27**, 558 (1963), *Kagaku Kogaku* (Abridged Edition), **2**, 18 (1964).
9) Nagata, S., K. Hashimoto, N. Taneda, Y. Horiguchi, N. Suzuki and T. Akita: *Kagaku Kogaku* (*Chem. Eng., Japan*), **29**, 597 (1965), *Kagaku Kogaku* (Abridged Edition) **4**, 49 (1966).
10) Oki. Y., E. Oshima, H. Inoue and S. Yagi: *Kagaku Kogaku* (*Chem. Eng., Japan*), **30**, 341 (1966).
11) Rosenberg, D.U., P.L. Durrill and E.H. Spencer: *Brit. Chem. Eng.*, **7**, 186 (1962).
12) Schuler, R.W., V.P. Stallings and J.M. Smith: *Chem. Eng. Progr., Symposium Ser.*, **48**, No. 4, 19 (1952).
13) Smith, J.M.: "Chemical Engineering Kinetics", McGraw-Hill, N.Y. (1956)
14) Walas, S.M.: "Reaction Kinetics for Chemical Engineers", McGraw-Hill, N.Y., (1959).
15) Yoshida, F., D. Ramaswami and O.A. Hougen: *A.I. Ch. E. Journal*, **8**, 5 (1962).